

Randall-Sundrum model with a small curvature and dimuon production at the LHC

A.V. Kisselev*

Institute for High Energy Physics, 142281 Protvino, Russia

and

Department of Physics, Moscow State University, 119991 Moscow, Russia

Abstract

The p_{\perp} -distributions for the dimuon production at the LHC are calculated in the Randall-Sundrum scenario with a small curvature κ . The pp collisions at 7 TeV and 14 TeV are considered. The widths of massive graviton excitations are taken into account. It is found that the LHC discovery limit on 5-dimensional gravity scale M_5 is equal to 5.5 TeV for $\sqrt{s} = 7$ TeV and integrated luminosity 5 fb^{-1} . For $\sqrt{s} = 14$ TeV and integrated luminosities 30 fb^{-1} and 100 fb^{-1} , the search limits in the dimuon events are 12.0 TeV and 14.6 TeV, respectively. Contrary to the standard RS model, these limits are independent of κ , provided $\kappa \ll M_5$.

1 Extra dimension with the small curvature

The goal of the present paper is to estimate gravity effects in the dimuon production at the LHC in a scheme with a warp extra dimension, and to derive search limits on a fundamental 5-dimensional gravity scale M_5 .

The standard Randall-Sundrum (RS) model [1] is the theory with one extra dimension (ED) in a slice of the AdS_5 space-time. It predicts a series

*Electronic address: alexandre.kisselev@ihep.ru

of massive Kaluza-Klein (KK) resonances with the lightest one, m_1 , around one TeV. A lot of efforts were made in order to find effects coming from warped ED. The bounds on 5-dimensional Planck scale M_5 and/or m_1 were obtained both at the Tevatron [2] and recently at the LHC. In particular, high-mass dilepton [3], diphoton [4] and $t\bar{t}$ resonance events [5] were searched for in pp collisions at $\sqrt{s} = 7$ TeV with the ATLAS and CMS experiments (see also [6], [7]).

In the present paper we will study the RS scenario with the 5-dimensional Planck scale M_5 in the TeV region and *small curvature* [8]-[12]:¹

$$\kappa \ll M_5 . \quad (1)$$

In such a scheme, the background warped metric looks like

$$ds^2 = e^{2\kappa(\pi r_c - |y|)} \eta_{\mu\nu} dx^\mu dx^\nu + dy^2 . \quad (2)$$

Here $y = r_c \theta$ ($-\pi \leq \theta \leq \pi$) is the 5-th dimension coordinate, r_c is the size of the ED, $\eta_{\mu\nu}$ is the Minkowski metric. The points (x_μ, y) and $(x_\mu, -y)$ are identified, so one gets the orbifold S^1/Z_2 . The parameter κ defines the 5-dimensional scalar curvature of the AdS_5 space. In what follows, we will call it *curvature*.

We are interested in the RS scheme with two 3D branes with equal and opposite tensions located in 5-th dimension at the points $y = \pi r_c$ (called TeV brane) and $y = 0$ (called Plank brane). The SM fields are constrained to the TeV brane, while the gravity propagates in all five spatial dimensions.

It is necessary to note that metric (2) is chosen in such a way that 4-dimensional coordinates x^μ are Galilean on the TeV brane where all the SM fields live, since the warp factor is equal to unity at $y = \pi r_c$. Due to the warp factor in the metric (2), the gravity is strong on the Plank brane, while it is weak on the TeV brane.

By integrating 5-dimensional action in variable y , one can get an effective 4-dimensional action which, in its turn, leads to so-called *hierarchy relation* between the 5-dimensional *reduced* gravity scale \bar{M}_5 and *reduced* Planck mass \bar{M}_{Pl} :

$$\bar{M}_{Pl}^2 = \frac{\bar{M}_5^3}{\kappa} (e^{2\pi\kappa r_c} - 1) . \quad (3)$$

¹The ratio of the 5-dimensional scalar curvatures in our scheme \mathcal{R} to the scalar curvature in the standard RS scheme \mathcal{R}_0 is given by $\mathcal{R}/\mathcal{R}_0 \simeq (\kappa/\bar{M}_5)^3 \ll 1$.

The fundamental gravity scale M_5 (i.e., Planck scale in five dimensions) and reduced scale \bar{M}_5 are related as follows:

$$M_5 = (2\pi)^{1/3} \bar{M}_5 \simeq 1.84 \bar{M}_5 . \quad (4)$$

In order the hierarchy relation (3) to be satisfied, it is enough to take $r_c \kappa \simeq 8 \div 9.5$, that corresponds to $r_c \simeq 0.15 \div 1.8$ fm. In what follows, we choose \bar{M}_5 to be of the order of several TeV to tens TeV, while κ is allowed to vary from hundred MeV to tens GeV. Thus, no new parameters of the order of \bar{M}_{Pl} (as in the standard RS model [1], in which $\kappa \sim M_5 \sim M_{\text{Pl}}$) are introduced in our scheme.

From the point of view of a 4-dimensional observer located on the TeV brane, in addition to the massless graviton, there exists an infinite number of its Kaluza-Klein (KK) excitations, $G_{\mu\nu}^{(n)}$, with the masses

$$m_n = x_n \kappa, \quad n = 1, 2 \dots , \quad (5)$$

where x_n are zeros of the Bessel function $J_1(x)$, and n is the KK-number.

The interaction of the KK gravitons with the the SM fields on the TeV brane is described by the Lagrangian

$$\mathcal{L}_{int} = -\frac{1}{\bar{M}_{\text{Pl}}} T^{\mu\nu} G_{\mu\nu}^{(0)} - \frac{1}{\Lambda_\pi} T^{\mu\nu} \sum_{n=1}^{\infty} G_{\mu\nu}^{(n)} , \quad (6)$$

where $T^{\mu\nu}$ is the energy-momentum tensor of the SM fields. The parameter

$$\Lambda_\pi = \bar{M}_5 \left(\frac{\bar{M}_5}{\kappa} \right)^{1/2} \quad (7)$$

can be regarded as a physical scale on the TeV brane where all SM fields live.

The scalar field, radion, is omitted in the Lagrangian (6). In our scheme, it practically decouples from the SM fields since its coupling on the TeV brane is proportional to [8]

$$g_{\text{rad}}^2 \simeq 3 \cdot 10^{-4} \left(\frac{\kappa}{\text{GeV}} \right) \left(\frac{\text{TeV}}{\bar{M}_5} \right)^3 \text{TeV}^{-2} . \quad (8)$$

In particular, for $\kappa = 1$ GeV and $\bar{M}_5 = 1$ TeV, one gets $g_{\text{rad}} \sim 1/(100 \text{ TeV})$.

As for processes with a real or virtual production of the KK gravitons, the smallness of their coupling to the SM particles, $1/\Lambda_\pi$, is compensated by a

large number of real gravitons or by infinite tower of virtual KK excitations. As a result, a magnitude of the cross sections is defined by the scale \bar{M}_5 , not the scale Λ_π [8] (as an illustration, see (21)).

As it was already mentioned above, the 4-dimensional coordinates are Galilean on the TeV brane. Thus, a correct determination of the masses on this brane can be achieved [13]. In particular, observed masses coincide with their Lagrangian values and do not depend on a coordinate rescaling, if covariant equations and invariant distances are used [14].

The RS-like model under consideration has other interesting features. For instance, the spectrum of the KK gravitons (5) is very similar to that in the ADD model with one ED [15]. Moreover, all matrix elements can be formally obtained from corresponding matrix elements calculated in the ADD model with one *flat* extra dimension by using following replacements [8, 10]:

$$\bar{M}_{4+1} \rightarrow (2\pi)^{-1/3} \bar{M}_5, \quad R_c \rightarrow (\pi\kappa)^{-1}. \quad (9)$$

Here \bar{M}_{4+1} is a 5-dimensional reduced Planck scale, R_c being the radius of the compact flat dimension.

2 Gravitons in dimuon production at the LHC

In this section we will study a production of two muons with high transverse momenta in pp -collisions [16]:²

$$pp \rightarrow \mu^+ \mu^- + X. \quad (10)$$

We are interested in a possible excess in p_\perp -distribution of the final leptons coming from gravity interactions in 5-dimensional space-time with the small curvature. The theoretical framework was described in details in the previous section.

The dilepton production is a favourable process to look for gravity effects predicted by theories based on a space-time with more than four dimensions. The Tevatron data on p_\perp -distribution in dilepton production already provided us with bounds on parameters of these theories [17]. As for dilepton production at the LHC, the search for EDs resulted in new limits on so-called large EDs [18]. However, most efforts of ATLAS and CMS Collaborations

²The production of a lepton pair in pp (or $p\bar{p}$) collision is often called Drell-Yan process.

were made to search for massive resonances in such events predicted by theories with the warped metric (see, for instance, [3, 6]). The phenomenology of the RS model with the resonant KK spectrum in the TeV region can be found in [19]. The determination of the spin-2 RS gravitons against spin-1 and spin-0 resonances in lepton-pair production was done in [20].

The goal of this paper is to estimate gravity effects in the dimuon production at the LHC in the RS scenario with the small curvature [8]-[10]. The differential cross section of this process (10) is given by

$$\begin{aligned} \frac{d\sigma}{dp_{\perp}}(pp \rightarrow \mu^+ \mu^- + X) = 2p_{\perp} \sum_{a,b=q,\bar{q},g} \int \frac{d\tau \sqrt{\tau}}{\sqrt{\tau - x_{\perp}^2}} \int \frac{dx_1}{x_1} f_{a/p}(\mu^2, x_1) \\ \times f_{b/p}(\mu^2, \tau/x_1) \frac{d\hat{\sigma}}{d\hat{t}}(ab \rightarrow \mu^+ \mu^-), \end{aligned} \quad (11)$$

with the transverse energy of the muon pair equals to $2p_{\perp}$. Here $f_{a/p}(\mu^2, x_1)$ is the distribution of the parton of the type a in momentum fraction x_1 inside the proton taken at the scale μ . $d\hat{\sigma}/d\hat{t}$ denotes the cross section of the partonic subprocess $ab \rightarrow \mu^+ \mu^-$, which is described by the Mandelstam variables \hat{s} , \hat{t} and \hat{u} ($\hat{s} + \hat{t} + \hat{u} = 0$).

We introduced two dimensionless quantities,

$$\begin{aligned} x_{\perp} &= \frac{2p_{\perp}}{\sqrt{s}}, \\ \tau &= x_1 x_2, \end{aligned} \quad (12)$$

where x_2 is the momentum fraction of the parton b in (11). Without cuts, integration variables in (11) vary within the following limits

$$\begin{aligned} x_{\perp}^2 &\leq \tau \leq 1, \\ \tau &\leq x_1 \leq 1. \end{aligned} \quad (13)$$

After imposing kinematical cut, the integration region becomes more complicated (see Appendix A).

The contribution of the virtual gravitons to lepton pair production ($l = e$ or μ) comes from the quark-antiquark annihilation, $q \bar{q} \rightarrow G^{(n)} \rightarrow l^+ l^-$, and gluon-gluon fusion, $g g \rightarrow G^{(n)} \rightarrow l^+ l^-$. The corresponding partonic

cross sections are (see, for instance, Appendix A in [9])

$$\begin{aligned}\frac{d\hat{\sigma}}{d\hat{t}}(q\bar{q} \rightarrow l^+l^-) &= \frac{\hat{s}^4 + 10\hat{s}^3\hat{t} + 42\hat{s}^2\hat{t}^2 + 64\hat{s}\hat{t}^3 + 32\hat{t}^4}{1536\pi\hat{s}^2} |\mathcal{S}(\hat{s})|^2, \\ \frac{d\hat{\sigma}}{d\hat{t}}(gg \rightarrow l^+l^-) &= -\frac{\hat{t}(\hat{s} + \hat{t})(\hat{s}^2 + 2\hat{s}\hat{t} + 2\hat{t}^2)}{256\pi\hat{s}^2} |\mathcal{S}(\hat{s})|^2,\end{aligned}\quad (14)$$

where

$$\mathcal{S}(s) = \frac{1}{\Lambda_\pi^2} \sum_{n=1}^{\infty} \frac{1}{s - m_n^2 + i m_n \Gamma_n} \quad (15)$$

is the invariant part of the partonic matrix elements, with Γ_n being total width of the graviton with the KK number n and mass m_n [10]:

$$\Gamma_n = \eta m_n \left(\frac{m_n}{\Lambda_\pi} \right)^2, \quad \eta \simeq 0.09. \quad (16)$$

Note, because of the universal coupling of the KK gravitons to all SM fields, the function $\mathcal{S}(s)$ is the same for all processes mediated by s -channel virtual gravitons.

In the RS scenario with the small curvature, sum (15) was calculated analytically in [10]. At $s \sim \bar{M}_5 \gg \kappa$, it looks like

$$\mathcal{S}(s) = -\frac{1}{4\bar{M}_5^3\sqrt{s}} \frac{\sin 2A + i \sinh 2\varepsilon}{\cos^2 A + \sinh^2 \varepsilon}, \quad (17)$$

where

$$A = \frac{\sqrt{s}}{\kappa}, \quad \varepsilon = \frac{\eta}{2} \left(\frac{\sqrt{s}}{\bar{M}_5} \right)^3. \quad (18)$$

It is interesting to note that the magnitude of $\mathcal{S}(s)$ is defined by the fundamental gravity scale \bar{M}_5 , while the scale Λ_π , which is contained in the Lagrangian (6), did not appear in (17). Let us underline that only for $\varepsilon \gg 1$ we come to the expression which can be obtained by neglecting widths of the massive gravitons (*zero width approximation*):³

$$\text{Im } \mathcal{S}(\hat{s}) \simeq -\frac{1}{2\bar{M}_5^3\sqrt{\hat{s}}}, \quad \text{Re } \mathcal{S}(\hat{s}) \simeq 0. \quad (19)$$

³In fact, zero width approximation is justified if inequality $s \gtrsim 3.5 \bar{M}_5^2$ is satisfied [10]. Under this condition, $\text{Re } \mathcal{S}/\text{Im } \mathcal{S} < 0.05$.

In what follows, we will consider $\bar{M}_5 \geq 2(4)$ TeV for the LHC energy $\sqrt{s} = 7(14)$ TeV. In such a case, the parameter ε in (18) obeys inequality $\varepsilon < 2$, and one must use the exact formulae (17), (18) instead of the approximate expressions (19).⁴

As one can see from (17), the graviton spectrum in our model consists of very sharp resonances whose widths are proportional to $(\kappa/\bar{M}_5)^3$. The contribution from *one* resonance to the p_\perp -distribution can be estimated as follows (more details can be found in [12]):

$$\left. \frac{d\sigma(\text{grav})}{dp_\perp} \right|_{\text{one res}} \sim \frac{\kappa}{\bar{M}_5^3 \sqrt{s}}. \quad (20)$$

Since the total number of graviton resonances which contribute to the cross section is proportional to \sqrt{s}/κ , we obtain at fixed x_\perp

$$\frac{d\sigma(\text{grav})}{dp_\perp} \sim \frac{1}{\bar{M}_5^3}. \quad (21)$$

Let us stress that in our scheme the gravity cross sections *do not depend* on the curvature κ , provided $\kappa \ll \bar{M}_5$,⁵ in contrast to the RS model with the large curvature in which $\kappa \sim \bar{M}_5 \sim \bar{M}_{\text{Pl}}$ [1].

In order to obtain search limits for the LHC, we calculate contributions from s -channel graviton resonances to the p_\perp -distributions of the final muons for different values of 5-dimensional Planck scale \bar{M}_5 . We use the MSTW 2008 NNLO parton distributions [21], and convolute them with the partonic cross sections (14) in (11). The PDF scale is taken to be equal to the invariant mass of the muon pair, $\mu = M_{l+l-} = \sqrt{\hat{s}}$.

We also impose the cut on the lepton pseudorapidities which is used by ATLAS and CMS Collaborations in selecting dimuon events [6]:

$$|\eta| < 2.4. \quad (22)$$

The limits on variations of the variables τ and x_1 in (11), resulting from this cut, are derived in Appendix A.

The reconstruction efficiency of 85% is assumed for the muon events [22]. Note that this assumption is not very crucial for our scheme. For instance,

⁴Since a mean value of the partonic energy $\sqrt{\hat{s}}$ is less than the collision energy \sqrt{s} , an effective value of the parameter ε is even less than 1.

⁵Up to very small corrections of the type $O(\kappa/\bar{M}_5)$.

given the efficiency varies from 85% to 80%, the LHC search limits on \bar{M}_5 diminish by 1% only, due to the strong power-like dependence of the gravity cross section on \bar{M}_5 (21).⁶

In Fig. 1 and Fig. 2 we present the results of our calculations of gravity cross sections for the dimuon production at the LHC. The gravity mediated contributions to the cross sections do not include the SM contribution. The

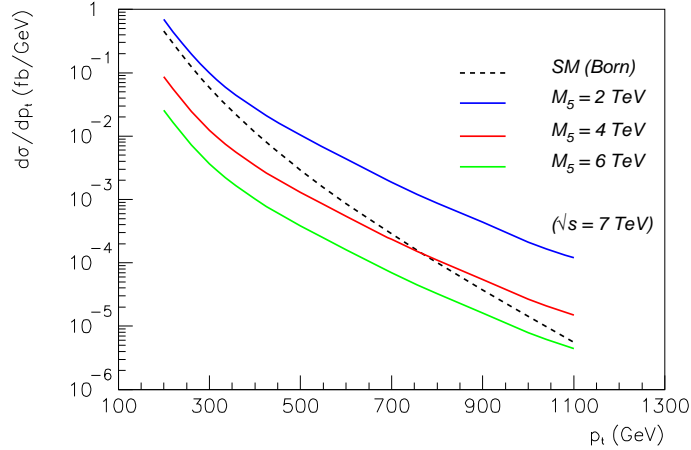


Figure 1: The KK graviton contribution to the dimuon production at the LHC for several values of 5-dimensional *reduced* Planck scale (solid curves) vs. SM contribution (dashed curve) at $\sqrt{s} = 7$ TeV.

ratios of the gravity induced cross sections to the SM one is shown in Fig. 3.

The differential cross section of the process under consideration is represented in the form:

$$d\sigma = d\sigma(\text{SM}) + d\sigma(\text{grav}) + d\sigma(\text{SM} - \text{grav}) , \quad (23)$$

where the last term comes from the interference between the SM and graviton interactions. Since the SM amplitude is pure real, while the real part of each graviton resonance is antisymmetric with respect to its central point, the interference term in (23) has appeared to be negligible in comparison with

⁶Namely, a significant variation of $d\sigma(\text{grav})/dp_{\perp}$ can be achieved by a relatively small variation of \bar{M}_5 .

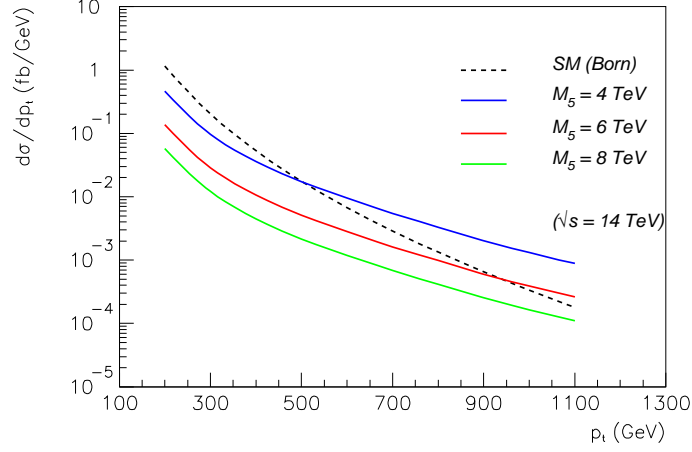


Figure 2: The same as in Fig. 1, but for the energy $\sqrt{s} = 14$ TeV.

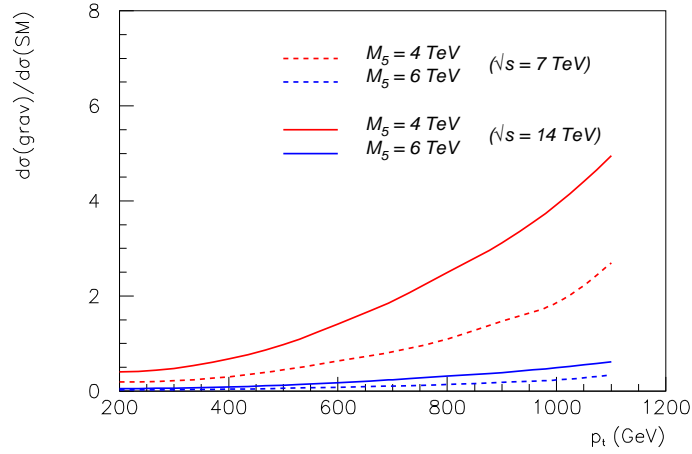


Figure 3: The ratio of the gravity induced cross sections to the SM dimuon cross section at the LHC as a function of the muon transverse momentum for several values of 5-dimensional *reduced* Planck scale.

the pure gravity contribution (the second term in (23)) *after integration* in partonic momenta. More details can be found in [12].

The next Fig. 4 demonstrates us that an ignorance of the graviton widths would be a *rough approximation*. As one can see, it results in very large suppression of the cross sections. The reason of this suppression lies partially in the fact that [12]

$$\frac{d\sigma(\text{grav})}{dp_{\perp}} \sim \frac{1}{p_{\perp}^3} \left(\frac{\sqrt{s}}{\overline{M}_5} \right)^3, \quad (24)$$

while in zero width approximation

$$\left. \frac{d\sigma(\text{grav})}{dp_{\perp}} \right|_{\text{zero width}} \sim \frac{1}{\overline{M}_5^3} \left(\frac{\sqrt{s}}{\overline{M}_5} \right)^3, \quad (25)$$

as one can derive it from formulae (11), (14) and (19).

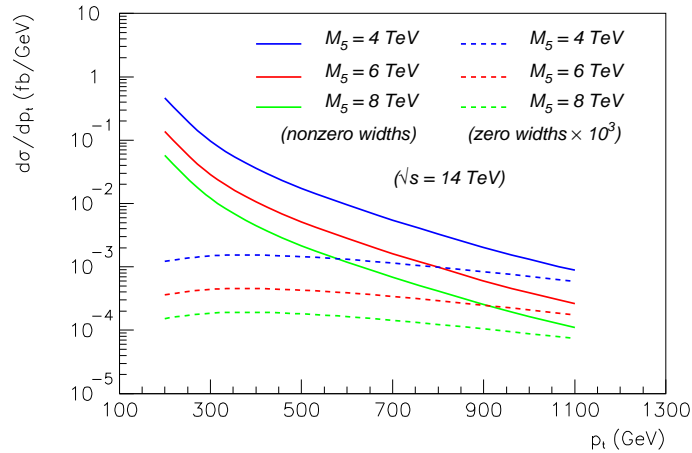


Figure 4: The contributions to the dimuon events from the KK gravitons with nonzero widths (solid curves) vs. contributions from zero width gravitons (multiplied by 10^3 , dashed curves) for the different values of the *reduced* 5-dimensional Planck scale.

To take into account higher order contributions, we use a K -factor 1.5 for the SM background,⁷ while a conservative value of $K = 1$ is taken for

⁷For the dimuon channel, the expected SM background consists of Z/γ^* , $t\bar{t}$ and diboson events (Z/γ^* being dominant), while ($W + \text{jets}$) and QCD background is negligible [23].

the signal. Let $N_S(N_B)$ be a number of signal (background) dimuon events with $p_\perp > p_\perp^{\text{cut}}$. Then we define the statistical significance $\mathcal{S} = N_S/\sqrt{N_B}$, and require a 5σ effect. In Fig. 5 the statistical significance is shown for $\sqrt{s} = 7$ TeV as a function of the transverse momentum cut p_\perp^{cut} and *reduced* 5-dimensional gravity scale \bar{M}_5 . Figs. 6 and 7 represent \mathcal{S} for the dimuon events at $\sqrt{s} = 14$ TeV.

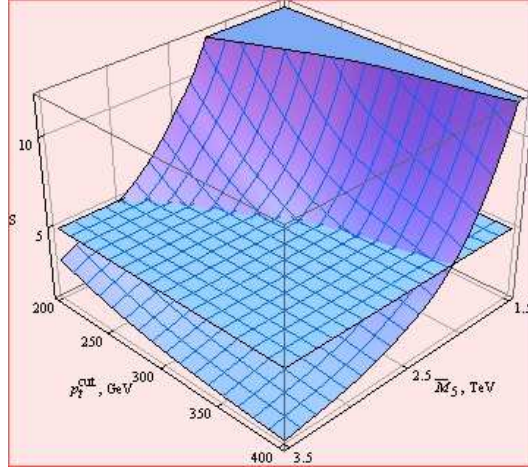


Figure 5: The statistical significance S for the dimuon production at the LHC for $\sqrt{s} = 7$ TeV and integrated luminosity 5 fb^{-1} as a function of the transverse momentum cut p_\perp^{cut} and *reduced* 5-dimensional gravity scale \bar{M}_5 . The plane $S = 5$ is also shown.

The authors of Ref. [9] proposed a search in the dilepton channel by cutting on the invariant masses M_{l+l-} above 2 TeV. They found a 5 sigma bound on $M_5 = 4$ TeV (without taking into account finite graviton widths). In our case, we have the lower bound on $M_{l+l-} = 2p_\perp$ and integrate in variable $\tau = M_{l+l-}^2/s$.

3 Conclusions and discussions

In the present paper the RS-like scenario with the small curvature of the space-time [8]-[10] is considered. In such a scheme, the reduced 5-dimensional Planck scale \bar{M}_5 can vary from few TeV to tens TeV, while the curvature κ

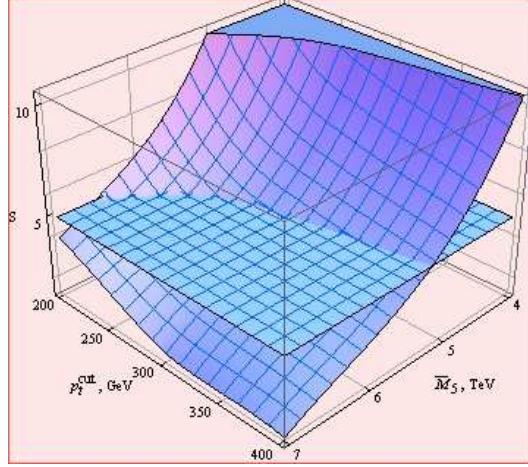


Figure 6: The same as in Fig. 5, but for $\sqrt{s} = 14$ TeV and integrated luminosity 30 fb^{-1} .

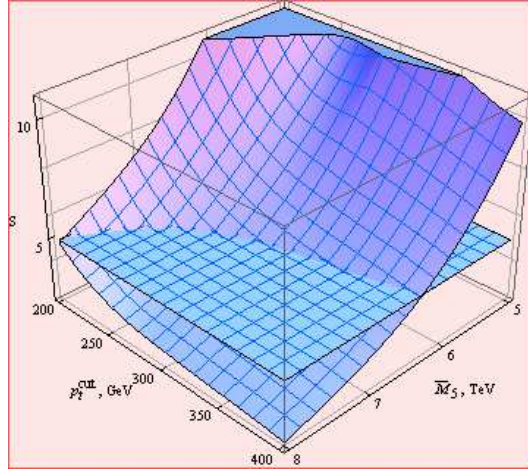


Figure 7: The same as in Fig. 5, but for $\sqrt{s} = 14$ TeV and integrated luminosity 100 fb^{-1} .

is allowed to vary from hundred MeV to few GeV (in fact, the only condition $\kappa \ll \bar{M}_5$ should be satisfied). The mass spectrum and experimental signature of the model are similar to those in the ADD model [15] with one flat extra dimension.

The p_\perp -distributions for the muon pairs production with high p_\perp at the LHC are calculated for the collision energies $\sqrt{s} = 7$ TeV and $\sqrt{s} = 14$ TeV (see Figs. 1-3). The importance of the account of the KK graviton widths is demonstrated (see Fig. 4). The statistical significance as a function of the *reduced* 5-dimensional Planck scale \bar{M}_5 and cut on the lepton transverse momentum p_\perp^{cut} is calculated (see Figs. 5-7).

By using these results, we can obtain the following discovery limit for the 7 TeV LHC and integrated luminosity of 5 fb^{-1} in the dimuon production:

$$M_5 = 5.5 \text{ TeV} . \quad (26)$$

Correspondingly, we obtain for the 14 TeV LHC:

$$M_5 = \begin{cases} 12.0 \text{ TeV} , & \mathcal{L} = 30 \text{ fb}^{-1} \\ 14.6 \text{ TeV} , & \mathcal{L} = 100 \text{ fb}^{-1} \end{cases} \quad (27)$$

In deriving (26) and (27), we used the relation $M_5 = (2\pi)^{1/3} \bar{M}_5$ (4).

It is important that these bounds on M_5 do not depend on the curvature κ , contrary to the standard RS model [1] in which estimated bounds on M_5 depend significantly on the value of the ratio $\kappa/\bar{M}_{\text{Pl}}$.

Previously, analogous bounds were obtained for the diphoton production at the Tevatron and 14 TeV LHC [12]. Recently, results on the dilepton production at very high luminosity (HL-LHC) were presented [24].

Our approach can be directly applied to the production of the *electron pairs* at the LHC. The only thing to do is to take into account that for electron samples the transition region $1.37 < |\eta| < 1.52$ ($1.44 < |\eta| < 1.57$) between the ECAL barrel and endcap calorimeters is usually excluded in the ATLAS (CMS) experiment, while the cuts $|\eta| < 2.47$ and $|\eta| < 2.5$ are imposed by the ATLAS and CMS experiments, respectively (see, for instance, [6]).

Acknowledgements

The author is indebted to A.G. Myagkov and S.V. Shmatov for useful discussions.

References

- [1] L. Randall and R. Sundrum, Phys. Rev. Lett. **83** (1999) 3370.
- [2] T. Aaltonen *et al.* (CDF Collaboration), Phys. Rev. Lett. **102** (2009) 091805; V.M. Abazov *et al.* (D0 Collaboration), Phys. Rev. Lett. **104** (2010) 241802.
- [3] G. Aad *et al.* (ATLAS Collaboration), Phys. Rev. Lett. **107** (2011) 272002; S. Chatrchyan *et al.* (CMS Collaboration), Phys. Lett. B. **714** (2012) 158.
- [4] G. Aad *et al.* (ATLAS Collaboration), Phys. Lett. B **70** (2012) 538; S. Chatrchyan *et al.* (CMS Collaboration), Phys. Rev. Lett. **108** (2012) 111801.
- [5] G. Aad *et al.* (ATLAS Collaboration, Eur. Phys. J. C **72** (2012) 2083.
- [6] S. Viel (for the ATLAS Collaboration), *Proc. of the XXXI International Conference on Physics in Collision*, Vancouver, BC Canada, August 28–September 1, 2011, arXiv:1111.2360; V. Timciuc (on behalf of the CMS Collaboration), *Proc. of the XXXI International Conference on Physics in Collision*, Vancouver, BC Canada, August 28–September 1, 2011, arXiv:1111.4528.
- [7] T.J. Orimoto (on behalf of the CMS Collaboration), EPJ Web of Conferences **28** (2012) 09010.
- [8] A.V. Kisselev and V.A. Petrov, Phys. Rev. D **71** (2005) 124032.
- [9] G. F. Giudice, T. Plehn and A. Strumia, Nucl. Phys. B **706** (2005) 455.
- [10] A.V. Kisselev, Phys. Rev. D **73** (2006) 024007.
- [11] A.V. Kisselev, V.A. Petrov and R.A. Ryutin, Phys. Lett. B **630** (2005) 100; A.V. Kisselev, JHEP **0703** (2007) 006.
- [12] A.V. Kisselev, JHEP **0809** (2008) 039.
- [13] E.E. Boos, Yu.A. Kubyshin, M.N. Smolyakov and I.P. Volobuev, Class. Quan. Grav. **19** (2002) 4591; Nucl. Phys. B **717** (2005) 9.

- [14] B. Grinstein, D.R. Nolte and W. Skiba, Phys. Rev. D **63** (2001) 105005.
- [15] N. Arkani-Hamed, S. Dimopoulos and G. Dvali, Phys. Lett. B **429** (1998) 263; I. Antoniadis, N. Arkani-Hamed, S. Dimopoulos and G. Dvali, Phys. Lett. B **436** (1998) 257; N. Arkani-Hamed, S. Dimopoulos and G. Dvali, Phys. Rev. D **59** (1999) 086004.
- [16] V.A. Matveev, R.M. Muradian and A.N. Tavkhelidze, JINR P2-4543 (Dubna, 1969), SLAC TRANS-009: JINR R2-4543 (June, 1969); S.D. Drell and T.M. Yan, SLAC-PUB-0755 (June, 1970), Phys. Rev. Lett. **25** (1970) 316, *errata* Phys. Rev. Lett. **25** (1970) 902.
- [17] T. Affolder *et al.* (CDF Collaboration), Phys. Rev. Lett. **84** (2000) 845. 10; B. Abbott *et al.* (D0 Collaboration), Phys. Rev. D **61** (2000) 032004, Phys. Rev. Lett. **84** (2000) 2792; V.M. Abazov *et al.* (D0 Collaboration), Phys. Rev. Lett. **100** (2008) 102002, *ibid* **104** (2010) 241802.
- [18] G. Aad *et al.* (ATLAS Collaboration), Phys. Lett. B **716** (2012) 122; S. Chatrchyan *et al.* (CMS Collaboration), JHEP **05** (2011) 085, Phys. Lett. B **711** (2012) 15.
- [19] H. Davoudiasl, J.L. Hewett and T.G. Rizzo, Phys. Rev. Lett. **84** (2000) 2080; Phys. Rev. D **63** (2001) 075004.
- [20] P. Osland, A.A. Pankov, A.V. Tsytrinov and N. Paver, Phys. Rev. D **78** (2008) 035008.
- [21] A.D. Martin, W.J. Stirling, R.S. Thorne and G. Watt, Eur. Phys. J. C **63** (2009) 189.
- [22] G. Aad *et al.* (ATLAS Collaboration), arXiv:1209.2535.
- [23] The ATLAS Collaboration, Proc. of the *47-th Rencontres de Moriond on Electroweak Interactions and Unified Theories*, La Thuile, Italy, 3-10 March 2012, arXiv:1111.2360.
- [24] A.V. Kisselev, *Talk presented at the CMS Workshop on Perspectives on Physics and on CMS at Very High Luminosity*, Alushta, Crimea, Ukraine, 28–31 May, 2012, arXiv:1208.3844.

Appendix A

In this section we will calculate the integration region in (11) in a case when a cut on final lepton (pseudo)rapidities is imposed. Let us consider a production of a lepton pair with high transverse momenta p_\perp in pp collision:

$$pp \rightarrow l^+ l^- + X, \quad l = e, \mu. \quad (\text{A.1})$$

In the c.m.s. of the initial protons, their 4-momenta are

$$p_{1,2}^\mu = \frac{\sqrt{s}}{2}(1, \vec{0}, \pm 1), \quad (\text{A.2})$$

where \sqrt{s} is the collision energy. Let us call this system *lab-system*, contrary to the c.m.s. of the final leptons. In what follows, we neglect the masses of the protons and leptons with respect to \sqrt{s} , as well as inner transverse momenta of the partons inside the protons with respect to p_\perp .

Let x_1, x_2 be momentum fractions of the partons q_1, q_2 inside the colliding protons. Then the 4-momenta of the final leptons are:

$$l_{1,2}^\mu = (l_{1,2}^0, \pm \vec{p}_\perp, l_{1,2}^\parallel), \quad (\text{A.3})$$

with

$$\begin{aligned} l_{1,2}^\parallel &= \frac{\sqrt{s}}{4} \left[(x_1 - x_2) \pm (x_1 + x_2) \sqrt{1 - \frac{x_\perp^2}{\tau}} \right], \\ l_{1,2}^0 &= \frac{\sqrt{s}}{4} \left[(x_1 + x_2) \pm (x_1 - x_2) \sqrt{1 - \frac{x_\perp^2}{\tau}} \right]. \end{aligned} \quad (\text{A.4})$$

The dimensional variables τ and x_\perp were defined in the main text (12). They obey kinematical inequalities (13). The invariant mass of the lepton pair is $\hat{s} = s x_1 x_2$.

In the c.m.s. of the final leptons (herein called *cm-system*), the proton momenta look like

$$\begin{aligned} p_1^\mu &= \frac{\sqrt{s}}{2} \left(\sqrt{\frac{x_2}{x_1}}, \vec{0}, \sqrt{\frac{x_2}{x_1}} \right), \\ p_2^\mu &= \frac{\sqrt{s}}{2} \left(\sqrt{\frac{x_1}{x_2}}, \vec{0}, -\sqrt{\frac{x_1}{x_2}} \right), \end{aligned} \quad (\text{A.5})$$

while the parton momenta are

$$q_{1,2}^\mu = \frac{\sqrt{s}}{2} (\sqrt{x_1 x_2}, \vec{0}, \pm \sqrt{x_1 x_2}) . \quad (\text{A.6})$$

Correspondingly, the momenta of the leptons looks like

$$l_{1,2}^\mu = \left[\frac{\sqrt{s\tau}}{2}, \pm \vec{p}_\perp, \pm \frac{\sqrt{s\tau}}{2} \sqrt{1 - \frac{x_\perp^2}{\tau}} \right] . \quad (\text{A.7})$$

Note, since the lab-system and cm-system are related by a Lorentz boost along the beam axis, the partons momentum fractions remains the same in both systems.

Let us turn to the lab-system. The rapidity of the lepton pair in this system is equal to $(1/2) \ln(x_1/x_2)$. This means that the lepton rapidities are given by

$$\begin{aligned} y_1 &= \ln \left[\frac{x_1}{x_\perp} \left(1 + \sqrt{1 - \frac{x_\perp^2}{\tau}} \right) \right] , \\ y_2 &= -\ln \left[\frac{x_2}{x_\perp} \left(1 + \sqrt{1 - \frac{x_\perp^2}{\tau}} \right) \right] . \end{aligned} \quad (\text{A.8})$$

We are interested in the production of the leptons with the high momenta ($p_\perp \geq 200$ GeV). That is why, in order to estimate the integration region in (11), one can safely impose a cut on lepton *rapidities* $y_{1,2}$, instead of using cut on their *pseudorapidities*:⁸

$$|y_{1,2}| \leq y_{\text{cut}} . \quad (\text{A.9})$$

This bound is equivalent to the following inequalities:

$$A^{-1} \leq \frac{x_1}{\sqrt{\tau}} \leq A , \quad (\text{A.10})$$

where

$$A = \frac{x_\perp \exp(y_{\text{cut}})}{\sqrt{\tau} + \sqrt{\tau - x_\perp^2}} . \quad (\text{A.11})$$

⁸Remember that the rapidity is defined as $y = (1/2) \ln[(E + p_z)/(E - p_z)]$, while the pseudorapidity $\eta = (1/2) \ln[(p + p_z)/(p - p_z)] = -\ln[\tan(\theta/2)]$. For a relativistic particle ($p \gg m$), one gets $y \simeq \eta$ for $\theta \gg m/p$.

In order to get a non-zero integration region for x_1 , one must take $A \geq 1$. It leads to

$$\tau \leq x_{\perp}^2 \cosh^2 y_{\text{cut}} . \quad (\text{A.12})$$

The inequalities (A.10) and (A.12) must be treated simultaneously with the inequalities (13). Depending on values of x_{\perp} , the integration region splits into several parts:

1. $0 \leq x_{\perp} \leq \exp(-y_{\text{cut}})$. In this case:

$$\begin{aligned} x_{\perp}^2 &\leq \tau \leq x_{\perp}^2 \cosh^2 y_{\text{cut}} , \\ \sqrt{\tau} A^{-1} &\leq x_1 \leq \sqrt{\tau} A . \end{aligned} \quad (\text{A.13})$$

2. $\exp(-y_{\text{cut}}) < x_{\perp} \leq (\cosh y_{\text{cut}})^{-1}$. Variables τ, x_1 run two subregions:

$$\begin{aligned} x_{\perp}^2 &\leq \tau < \tau_0 , \\ \tau &\leq x_1 \leq 1 , \end{aligned} \quad (\text{A.14})$$

and

$$\begin{aligned} \tau_0 &\leq \tau \leq x_{\perp}^2 \cosh^2 y_{\text{cut}} , \\ \sqrt{\tau} A^{-1} &\leq x_1 \leq \sqrt{\tau} A . \end{aligned} \quad (\text{A.15})$$

Here we introduced the notation:⁹

$$\tau_0 = \frac{x_{\perp} \exp(-y_{\text{cut}})}{2 - x_{\perp} \exp(y_{\text{cut}})} . \quad (\text{A.16})$$

3. $(\cosh y_{\text{cut}})^{-1} < x_{\perp} \leq 1$. In this case, variables τ, x_1 run the region (13).

Without cuts on rapidities (formally, in the limit $y_{\text{cut}} \rightarrow \infty$), the full kinematically allowed region (13) is restored.

⁹Note that $x_{\perp}^2 \leq \tau_0 \leq x_{\perp}^2 \cosh^2 y_{\text{cut}}$ for the values of x_{\perp} under consideration.